JOURNAL OF Materials CHEMISTRY

A novel synthesis approach to transition metal boracites†

Jing Ju,[a] Hongmei Li,[a] Yingxia Wang,[a] Jianhua Lin*[a] and Cheng Dong[b]

[a]*State Key Laboratory of Rare Earth Materials Chemistry and Applications, College of Chemistry and Molecular Engineering, Peking University, Beijing 100871, P. R. China. E-mail: jhlin@chem.pku.edu.cn; Fax: 8610-62751708; Tel: 8610-62751715*
[b]*Institute of Physics, Chinese Academy of Sciences, Beijing 100080, P. R. China*

Received 17th October 2001, Accepted 13th February 2002
First published as an Advance Article on the web 15th April 2002

Five halogen boracites, $Mn_3B_7O_{13}Cl$, $Co_3B_7O_{13}Cl$, $Ni_3B_7O_{13}Cl$, $Cu_3B_7O_{13}Cl$, $Zn_3B_7O_{13}I$, have been synthesized by reaction of transition metal halides and boric acid at low temperature in the flux of boric acid. X-ray powder diffraction and chemical analysis of the halogen content show that the products are indeed stoichiometric halogen boracites, indicating that the proposed synthesis procedure is a convenient and promising way to the halogen boracites.

Introduction

Boracites form a family of compounds with the general formula $M_3B_7O_{13}X$ (M–X), where M can be Mg, Cr, Mn, Fe, Co, Ni, Cu, Zn or Cd and X can be F, Cl, Br, I, OH, NO_3.[1–3] Monovalent cation Li or divalent chalcogen anion, S, Se or Te[1,4] may also form boracite compounds; in such cases, the extra charge introduced might be compensated by oxygen vacancies as suggested by Fouassier *et al.*[5] Boracites, in particular the halogen boracites, exhibit unusual ferroelectric, magnetic, dynamic and structural properties, which have attracted considerable interest in the materials science community.[6–12] One of the interesting observations was the direct coupling between the spontaneous electric polarization and magnetization in $Ni_3B_7O_{13}I$, *i.e.* the orientation of the electric polarization can be reversed by switching the magnetization through 90° and *vice versa*.[9,13–15] This phenomenon raised a fundamental question about the coupling between the magnetic moment and the electric polarization, as well as any potential applications of this phenomenon. Halogen boracites were mostly synthesized by the vapor transport method; this method has been very successful particularly for growth of single crystals.[16,17] Other techniques, such as sol–gel processes[4] and hydrothermal methods,[1] were also studied. Hydrothermal synthesis is a convenient technique, which has been widely used for many systems, such as zeolites, and it was this technique that established the existence of the chalcogen, hydroxyl and lithium boracites.[18–21] However, the hydrothermal method is not suitable for halogen boracites. A recent study showed[3] that the products of the hydrothermal reaction are mainly hydroxyl boracites, even though the starting materials contained sufficient halogen anions. Recently, we have demonstrated that molten boric acid is a suitable reaction medium for polyborates and, a number of new rare earth polyborates, which can not be synthesized by conventional solid state reactions or hydrothermal reactions, were successfully obtained.[22] In this paper, we will show that this is a simple and clean approach to halogen boracites.

†Electronic supplementary information (ESI) available: selected bond distances and angles for $Co_3B_7O_{13}Cl$ and $Cu_3B_7O_{13}Cl$, refined atomic coordinates for $Cu_3B_7O_{13}Cl$. See http://www.rsc.org/suppdata/jm/b1/b109461k/

Experimental

General procedure

All chemicals used are commercially available without further purification. X-ray powder diffraction data were recorded on a Rigaku D/Max-2000 diffractometer at 50 kV, 100 mA for Cu Kα. The morphology of the crystals was investigated with a scanning electron microscope (SEM; AMRAY 1910 FE). Magnetic susceptibility measurements were performed on a SQUID magnetometer at 5 kOe from 5 to 300 K.

Synthesis procedure

To examine the effectiveness of the new synthesis procedure for boracite systems, five different boracites, $Co_3B_7O_{13}Cl$, $Cu_3B_7O_{13}Cl$, $Ni_3B_7O_{13}Cl$, $Mn_3B_7O_{13}Cl$ and $Zn_3B_7O_{13}I$, were synthesized with the molten boric acid flux method. Since synthesis procedures are rather similar, we will only address the experimental details on $Co_3B_7O_{13}Cl$, while the experimental conditions for the other boracites are summarized in Table 1. $Co_3B_7O_{13}Cl$ was synthesized by using $CoCl_2{\cdot}6H_2O$ and H_3BO_3 as the starting materials. A Teflon autoclave was charged

Table 1 Reaction conditions and products of the synthesis of $M_3B_7O_{13}X$ by using boric acid flux method

Metal halide	MX_2/H_3BO_3 (molar ratio)	T/°C	Time/d	Product	Yield[a] (%)	Halogen (wt%) Exp	Halogen (wt%) Calc
$CoCl_2{\cdot}6H_2O$	1/2–1/15	240	2	$Co_3B_7O_{13}Cl$	85	7.3(2)	7.15
$CoCl_2{\cdot}6H_2O$	1/2–1/15	270	2	$Co_3B_7O_{13}Cl$	95		
$NiCl_2{\cdot}6H_2O$	1/3–1/5	270	3	$Ni_3B_7O_{13}Cl$	50	7.2(2)	7.16
$NiCl_2{\cdot}6H_2O$	1/3–1/5	300	3	$Ni_3B_7O_{13}Cl$	75		
$MnCl_2{\cdot}4H_2O$	1/3–1/8	240	4	$Mn_3B_7O_{13}Cl$	80		
$CuCl_2{\cdot}2H_2O$	1/3–1/8	240	4	$Cu_3B_7O_{13}Cl$	90	7.4(2)	6.95
ZnI_2	1/3–1/8	240	4	$Zn_3B_7O_{13}I$	80	20.4(4)	20.92

[a]The calculation of the reaction yield was carried out under the condition that the MX_2/H_3BO_3 molar ratio was 1/3.

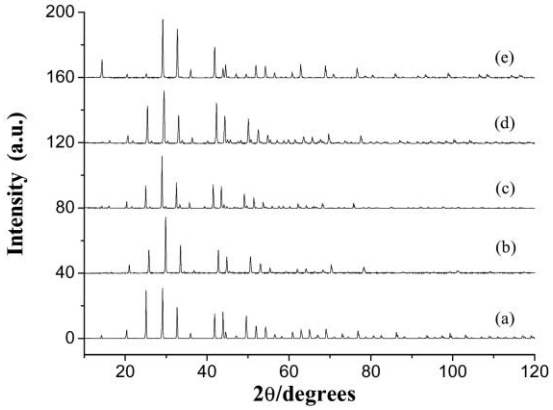

Fig. 1 X-ray powder diffraction of the boracites: (a) $Co_3B_7O_{13}Cl$; (b) $Cu_3B_7O_{13}Cl$; (c) $Mn_3B_7O_{13}Cl$; (d) $Ni_3B_7O_{13}Cl$; and (e) $Zn_3B_7O_{13}I$.

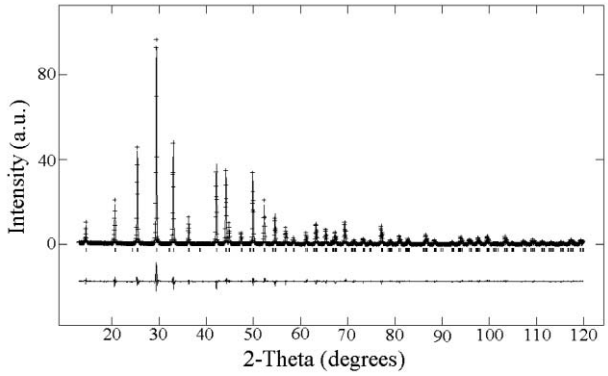

Fig. 2 Observed (+), calculated (line) and difference (bottom line) profiles of X-ray powder patterns of $Co_3B_7O_{13}Cl$ as a result of the Rietveld analysis. Tick marks indicate the positions of possible reflections.

with $CoCl_2{\cdot}6H_2O$ (1.1896 g, 5 mmol) and H_3BO_3 (4.6373 g, 75 mmol), and the mixture was heated to 240 °C or 270 °C for 2 days. The product, isolated by dissolving the excess boric acid in water, is a purple, well-crystallized powder. It is worth emphasizing that the preparation of these boracites was done merely in boric acid flux without using any additional water or other solvent that is significantly different from typical hydrothermal synthesis.

The phase purity of the synthesized boracites was examined by powder X-ray diffraction and, it was confirmed that all the products are single phases. Halogen content in the products, except $Mn_3B_7O_{13}Cl$, was analyzed using the Mohr method[23] and the experimental and calculated values are listed in Table 1. The solution of $Mn_3B_7O_{13}Cl$ has a red color; therefore, the Mohr method can not be used for this compound.

Results and discussion

The synthesis reaction of boracites in molten boric acid is simple and straightforward. Boric acid melts at about 170 °C; it condenses to metaboric acid and then to boron oxide above the melting point in an open vessel. In the closed system, the presence of transition metal halide induces the dehydration and polymerization reaction of boric acid, which results in direct formation of boracites. Taking the cobalt chloride as a sample, the reaction can be expressed as:

$$3CoCl_2 + 7H_3BO_3 \xrightarrow{240\ ^\circ C} Co_3B_7O_{13}Cl + 5HCl + 8H_2O \quad (1)$$

The influence of reaction temperature and the M/B ratio was examined for all of the five boracites under study, which are summarized in Table 1. It seems that the reaction should be carried out above 240 °C; below which the reaction was not completed or no reaction occurred. The reaction temperature also exhibits a strong influence on the yield of the reaction. It can be seen from Table 1 that the yield of $Co_3B_7O_{13}Cl$ is about 85% at 240 °C, which increases to about 95% at 270 °C. Similar results were obtained for $Ni_3B_7O_{13}Cl$ (50% and 75% at 270 °C and 300 °C, respectively). The M/B ratio in the starting materials does not seem to have a significant influence on the reaction and, it was found that the single-phase products can be obtained with an M/B ratio from 1/2 to 1/15.

Fig. 1 shows the X-ray diffraction patterns of the transition metal boracites obtained by using this method. All of the products are single phase and crystallize with the boracite structure. It is well known that boracites undergo structural phase transition from a cubic structure ($F\bar{4}3c$) to an orthorhombic structure[1] at low temperature, which further transforms to rhombohedral or monoclinic structure at lower temperatures. The transition temperatures vary for different compounds; for example, the transition temperatures from cubic to orthorhombic structure vary from 60 to 800 K for the halogen boracites. Under the present conditions, $Co_3B_7O_{13}Cl$ crystallizes in the $Fe_3B_7O_{13}Cl$ type structure in space group $R3c$.[24] However, the deviation of the $Co_3B_7O_{13}Cl$ structure from cubic symmetry is so small that it could not be resolved even by careful refinement of the lattice constants; therefore the structure of $Co_3B_7O_{13}Cl$ has not yet been fully determined.[25] To identify the structure distortion from cubic symmetry, the structure of Co–Cl boracite was refined by using both cubic and rhombohedral structure models. It turned out that only the rhombohedral structure fits the X-ray powder diffraction pattern. Fig. 2 shows the profile fit of the X-ray diffraction pattern to the rhombohedral structure model. In contrast, a large deviation of the reflection intensities was observed for the cubic structure model. Table 2 contains the crystallographic

Table 2 Crystallographic data of $Co_3B_7O_{13}Cl$ and $Cu_3B_7O_{13}Cl$

Molecular formula	$Co_3B_7O_{13}Cl$	$Cu_3B_7O_{13}Cl$
Formula weight	2975.109	1996.266
Crystal system	Rhombohedral	Orthorhombic
Space group	$R3c$ (No. 161)	$Pca21$ (No. 29)
Unit cell dimension	a = 8.5507(1) Å	a = 8.4767(1) Å
		b = 8.4479(1) Å
	c = 20.9685(1) Å	c = 11.9634(1) Å
	V = 1327.689(12) Å^3	V = 856.669(26) Å^3
Z	6	4
Refined occupation factor of the Cl position	(6a) Occ. = 0.99(1)	(4a) Occ. = 1.00(1)
Density (calculated)	3.719 g cm^{-3}	3.957 g cm^{-3}
X-ray diffraction	Rigaku D/max-2000 13–120°, FT mode, 0.01° step^{-1}, 2 s step^{-1}	Rigaku D/max-2000 10–120°, FT mode, 0.02° step^{-1}, 2 s step^{-1}
Structure solution	Direct method, Sirpow 92	Direct method, Sirpow 92
Structure refinement	GSAS, Rietveld refinement	GSAS, Rietveld refinement
Residual value	R_p = 0.098	R_p = 0.023
	R_{wp} = 0.127	R_{wp} = 0.032

Table 3 Refined atomic coordinates of $Co_3B_7O_{13}Cl$

Atom	Wyckoff position	x	y	z	$U_i/U_e \times 100$
Co1	18b	0.1489(7)	0.2985(1)	0.3250(1)	0.62(2)
Cl1	6a	0.0	0.0	0.2629(1)	2.1(2)
B1	18b	0.1670(28)	0.8348(28)	0.0799(8)	1.2(2)
B2	18b	0.0886(34)	0.8952(33)	0.9734(6)	1.2(2)
B3	6a	0.0	0.0	0.0967(9)	1.2(2)
O1	6a	0.0	0.0	0.9891(5)	0.25(4)
O2	18b	0.8349(9)	0.0053(9)	0.0989(4)	0.25(4)
O3	18b	0.2881(11)	0.2619(15)	0.9619(4)	0.25(4)
O4	18b	0.1970(11)	0.9772(10)	0.9091(4)	0.25(4)
O5	18b	0.6925(11)	0.7715(9)	0.0180(4)	0.25(4)

Table 4 Lattice parameter of $M_3B_7O_{13}X$ boracites[a]

Space group	Sample	a/Å	b/Å	c/Å	R_{prof} (%)	Color of crystals
$Pca2_1$	Mn–Cl	8.676	8.683	12.292	6.71	White
$Pca2_1$	Cu–Cl	8.476	8.448	11.963	2.64	Straw yellow
$Pca2_1$	Ni–Cl	8.497	8.494	12.028	3.15	Orange–brown
$Pca2_1$	Zn–I	8.589	8.583	12.154	5.15	White
$R3c$	Co–Cl	8.551	8.551	20.969	6.67	Purple

[a]The lattice constants were refined with a full-profile refinement by using EXTRA.[29]

data and the coordinate parameters are listed in Table 3. The crystal structures of the other boracites, Mn–Cl, Cu–Cl and Ni–Cl, were known[26–28] and the lattice constants of the Mn–Cl, Cu–Cl and Ni–Cl samples obtained with the flux method agree

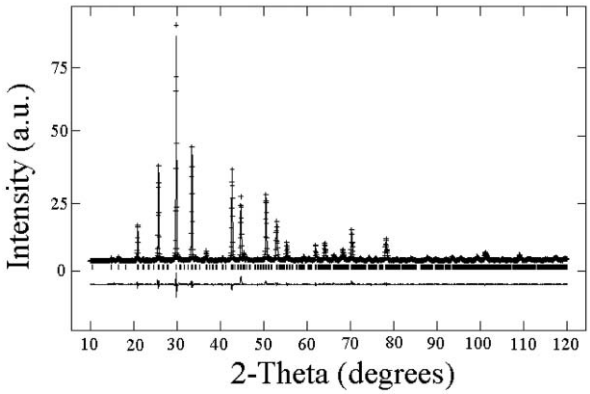

Fig. 3 Observed (+), calculated (line) and difference (bottom line) profiles of X-ray powder patterns of $Cu_3B_7O_{13}Cl$ as a result of the Rietveld analysis. Tick marks indicate the positions of possible reflections.

well with previous reports. Zn–I also crystallizes in $Pca2_1$ symmetry and the refined lattice constants are also listed in Table 4.

It is known that the hydrothermal method yielded mostly hydroxyl boracites rather than halogen boracites.[3,18] In boric acid flux, there is considerable amount of water generated as indicated in eqn. (1). To confirm that the products are halogen boracites, the halogen content was analyzed by chemical analysis using the Mohr method, which exclusively shows that the products are stoichiometric halogen boracites $M_3B_7O_{13}X$. For further confirmation of the presence of halogen in the

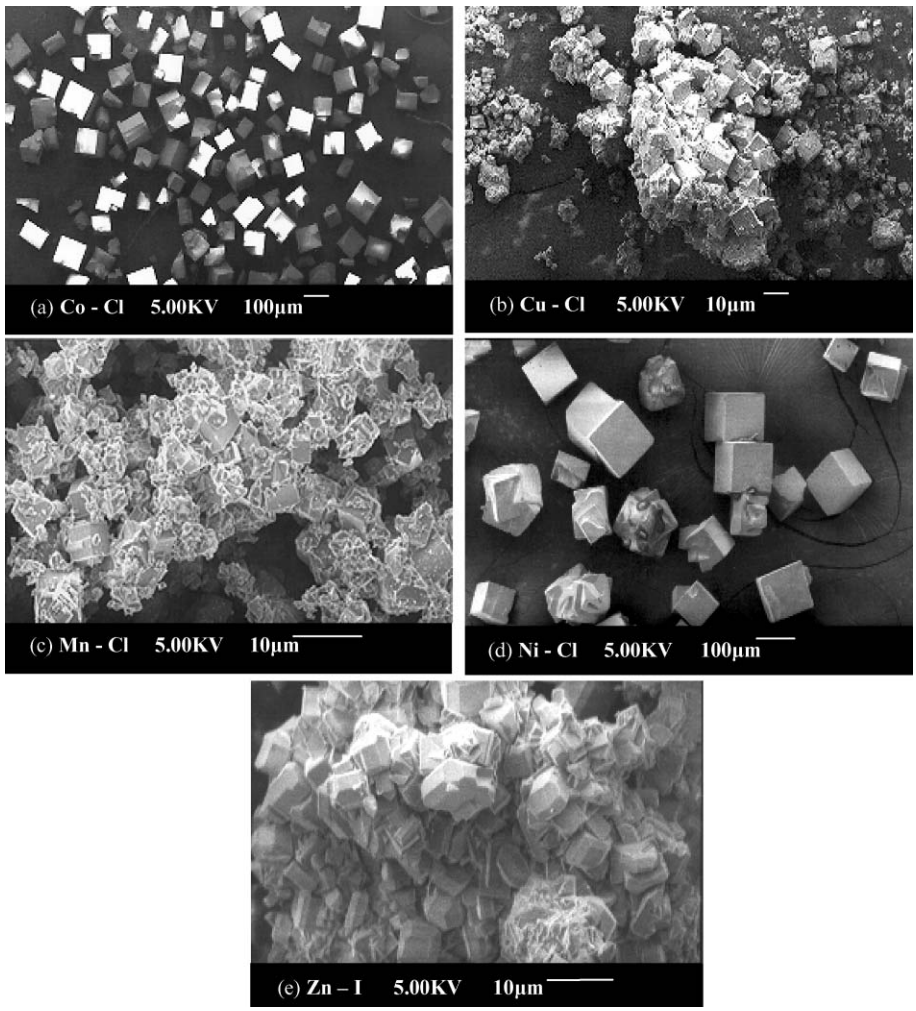

Fig. 4 SEM of the boracites: (a) $Co_3B_7O_{13}Cl$; (b) $Cu_3B_7O_{13}Cl$; (c) $Mn_3B_7O_{13}Cl$; (d) $Ni_3B_7O_{13}Cl$; and (e) $Zn_3B_7O_{13}I$.

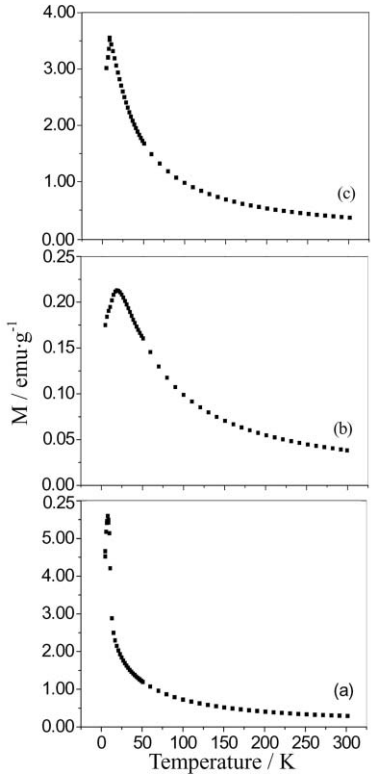

Fig. 5 Temperature dependence (between 5 and 300 K) of the magnetization M (emu g^{-1}) of: (a) $Co_3B_7O_{13}Cl$; (b) $Cu_3B_7O_{13}Cl$; and (c) $Mn_3B_7O_{13}Cl$, induced in a field of $H = 5$ kOe.

product, we performed additional Rietveld refinement on $Cu_3B_7O_{13}Cl$, in view of the fact that X-ray diffraction is capable of differentiating Cl and O in the structure. The refinement showed that the Cl position in $Cu_3B_7O_{13}Cl$ is indeed fully occupied (1.00(1)). As shown in Fig. 3, the X-ray diffraction pattern fits the orthorhombic structure model of $Cu_3B_7O_{13}Cl$ fairly well. Table 2 lists the crystallographic data of the refinement.

The boric acid flux method produces fairly good polycrystalline boracites. Fig. 4 shows the SEM images of the halogen boracites by using this method. Most of the products crystallize in regular cubic-like-shape of about 10 μm in size. For the Cu–Cl, Mn–Cl and Zn–I systems, smaller particles were also formed, which aggregate on the surface of the large crystals; nevertheless, they are all single-phase products of the halogen boracites.

The magnetic susceptibility shows typical Curie–Weiss behavior at high temperature for the $Mn_3B_7O_{13}Cl$, $Co_3B_7O_{13}Cl$ and $Cu_3B_7O_{13}Cl$ samples prepared by the boric acid flux method. At low temperature, antiferromagnetic interaction occurs for each of the three chloroboracites. Fig. 5 shows the magnetization of these compounds. The effective magnetic moments calculated from the high temperature data are 9.21, 8.28 and 3.19 μ_B for the Mn–Cl, Co–Cl and Cu–Cl boracites respectively. Compared with the spin-only value, the effective moment of Co–Cl boracite is a little bit higher, which was attributed to the weak ferromagnetic interaction observed in this system.[30] While for the Mn–Cl and Cu–Cl boracites, the effective moment agrees reasonably well to that of spin-only value.

In conclusion, it has been demonstrated that reaction of transition metal halides with boric acid in molten boric acid flux is a convenient and promising method to the halogen boracites. By using this technique, five different boracites, $Co_3B_7O_{13}Cl$, $Cu_3B_7O_{13}Cl$, $Mn_3B_7O_{13}Cl$, $Ni_3B_7O_{13}Cl$ and $Zn_3B_7O_{13}I$, were obtained as single phases. All of the chemical analysis and structural characterization supported the formation of halogen boracites. The simplicity, mild reaction conditions, as well as the stoichiometric products of this process may provide an alternative synthesis route for transition metal boracites in research or manufacturing.

Acknowledgement

We are thankful for the financial support from NSFC.

References

1 R. J. Nelms, *J. Phys. C: Solid State Phys.*, 1974, **7**, 3840.
2 T. A. Bither and H. S. Young, *J. Solid State Chem.*, 1974, **10**, 302.
3 U. Werthmann, H. Gies, J. Glinnemann and Th. Hahn, *Z. Kristallogr.*, 2000, **215**, 393.
4 T. Nagase, K. Sakane and H. Wada, *J. Sol–Gel Sci. Technol.*, 1998, **13**(1–3), 223.
5 C. Fouassier, A. Levasseur, J. C. Joubert, J. Muller and P. Hagenmuller, *Z. Anorg. Allg. Chem.*, 1970, **375**, 202.
6 P. Tolédamo, H. Schmid, M. Clin and J.-P. Rivera, *Phys. Rev. B*, 1985, **32**, 6006.
7 H. Schmid, *Ferroelectrics*, 1994, **162**, 317.
8 E. Burzo, in *Landolt-Börnstein, Numerical Data and Functional Relationships in Science and Technology, New Series*, ed. O. Madelung, Group III, Solid State Physics Vol. 27, Subvolume h, ed. H. P. J. Wijn, Springer, Berlin, 1993, p. 128.
9 H. Schmid, *Ferroelectrics*, 1999, **221**, 9.
10 B. B. Krichevtsov, A. A. Rzhevskii and H.-J. Weber, *Phys. Rev. B*, 2000, **61**, 10084.
11 S. Y. Mao, H. Schmid, G. Triscone and J. Muller, *J. Magn. Magn. Mater.*, 1999, **195**, 65.
12 W. Schnelle, E. Gmelin, O. Crottaz and H. Schmid, *J. Therm. Anal. Calorim.*, 1999, **56**, 365.
13 E. Ascher, H. Rieder, H. Schmid and H. Stössel, *J. Appl. Phys.*, 1966, **37**, 1404.
14 Y. Iguchi and K. Kohn, *Ferroelectrics*, 1992, **137**, 225.
15 M. Clin, J.-P. Rivera and H. Schmid, *Ferroelectrics*, 1990, **108**, 207.
16 H. Schmid, *J. Phys. Chem. Solids*, 1965, **26**, 973.
17 H. Schmid and H. Tippmann, *J. Cryst. Growth*, 1979, **46**, 273.
18 J. C. Joubert, J. Muller, C. Fouassier and A. Levasseur, *Krist. Tech.*, 1971, **6**, 65.
19 J. C. Joubert, J. Muller, M. Pernet and B. Ferrand, *Bull. Soc. Fr. Mineral. Cristallogr.*, 1972, **95**, 68.
20 A. Levasseur, C. Fouassier and P. Hagenmuller, *Mater. Res. Bull.*, 1971, **6**, 15.
21 W. Jeitschko and T. A. Bither, *Z. Naturforsch., B*, 1972, **27**, 1423.
22 P. C. Lu, Y. X. Wang, J. H. Lin and L. P. You, *Chem. Commun.*, 2001, 1178.
23 K. A. Li, X. Z. Ye and S. M. Jiao, in *Fundamental analysis chemistry lab*, ed. X. Q. Duan, Peking University, Beijing, 2nd edn, 1998, p. 192.
24 M.-E. Mendoza-Alvarez, K. Yvon, W. Depmeier and H. Schmid, *Acta Crystallogr., Sect. C*, 1985, **41**, 1551.
25 H. Schmid, *Phys. Status Solidi*, 1970, **37**, 209.
26 F. Kubel, *Z. Kristallogr.*, 1996, **211**, 924.
27 Y. Uesu, J. Kobayashi, I. Anjoh and H. Schmid, *Ferroelectrics*, 1978, **20**, 167.
28 F. Kubel, *Acta Crystallogr., Sect. C*, 1992, **48**, 1167.
29 A. Altomare, M. C. Burla, G. Cascarana, C. Glacovazzo, A. Guagliardi, A. G. G. Moliterni and G. Polidiori, *J. Appl. Crystallogr.*, 1995, **28**, 842.
30 M. S. Kumar, J.-P. Rivera, Z. G. Ye, S. D. Gentil and H. Schmid, *Ferroelectrics*, 1997, **204**(1–4), 57.